

Thermal Conductivity Measurements By Means of a New ‘Small Hot-Box’ Apparatus: Manufacturing, Calibration and Preliminary Experimental Tests on Different Materials

C. Buratti¹ · E. Belloni¹ · L. Lunghi¹ ·
M. Barbanera¹

Received: 16 November 2015 / Accepted: 22 February 2016
© Springer Science+Business Media New York 2016

Abstract The evaluation of the thermal performance building components requires a high level of accuracy. Windows, doors and thermal bridges are not homogeneous, and their thermal transmittance can be evaluated by means of Hot-Box, used for full-scale elements. For homogeneous materials and one-dimensional heat flux, the thermal conductivity can be easily measured through other experimental apparatuses, such as the guarded hot plate and the heat flow meters. This study presents a new experimental apparatus named Small Hot-Box, built at the University of Perugia. No European standards are available for this innovative facility, but it takes into account some prescriptions of EN ISO 8990 and EN ISO 12567; it was built for the evaluation of the thermal properties of small specimens. The apparatus was designed, built, and calibrated by means of preliminary measurements. It is composed of a hot and a cold side, and the external walls are made of thick insulation. The thermal conductivity can be calculated by two different methodologies: the Hot-Box and the thermal flux meter method. Preliminary calibrations were carried out and different materials with known thermal transmittance were tested. The aim is the development of a new experimental apparatus; guidance documents could be defined for the measurements methodology requirements.

✉ E. Belloni
belloni.unipg@ciriaf.it

C. Buratti
cinzia.buratti@unipg.it

L. Lunghi
lunghi.unipg@ciriaf.it

M. Barbanera
barbanera@crbnet.it

¹ Department of Engineering, University of Perugia, Via Duranti 93, 06125 Perugia, Italy

Keywords Building materials · Calibrated Hot-Box · Innovative experimental apparatus · Thermal conductivity

Nomenclature

A	Panel surface (m^2)
C	Thermal conductance ($\text{W}\cdot\text{m}^{-2}\cdot\text{K}^{-1}$)
e	Error (%)
H	Thermal transmittance ($\text{W}\cdot\text{m}^{-2}\cdot\text{K}^{-1}$)
λ	Thermal conductivity ($\text{W}\cdot\text{m}^{-1}\cdot\text{K}^{-1}$)
P	Power (W)
q	Heat flux ($\text{W}\cdot\text{m}^{-2}$)
R	Thermal resistance ($\text{m}^2\cdot\text{K}\cdot\text{W}^{-1}$)
s	Thickness (m)
T	Temperature ($^{\circ}\text{C}$)

Subscripts

a	Air
C	Cold side
e	External
f	Fans
g	Glass
H	Hot side
HB	Hot-Box method
i	Internal
I	Input
m	Mean
p	Panel
pol	Polyurethane
r	Resistance of the hot side
S	Surface
t	Total
tfm	Thermal flux meter method
w	Walls
wo	Wood

1 Introduction

Building energy consumption is increasing due to the improvement in living standards and indoor comfort and the building energy efficiency is a very urgent target [1–3]. As per the statistics provided by International Energy Agency, in Europe, energy consumptions in the residential, commercial and public service sectors constitute about 40 % of the total energy consumption [3]. Moreover, a relevant part of the buildings in Europe are old [4–6] with poor-quality insulation materials. In order to promote the

building energy efficiency, recent legislation, such as the EU Directive 2010/31 [7], has already been promulgated: the building components and materials deeply influence energy consumptions. The thermal properties of the building elements should be evaluated by means of accurate experimental methods that have been performed from research efforts all over the world. For the measurement of the thermal properties, several methods are available. Transient techniques are quite popular, due to their low measurement time. The transient hot-wire method is frequently used for the investigation of the thermal conductivity of fluids [8], while other techniques such as the hot-disk, hot-strip and hot-bridge are more commonly applied for solids [9–11].

The guarded hot plate is the most important and diffused method used for the estimation of the thermal conductivity of a homogeneous or multilayer material [12–14]. Some important studies for the characterization of thermal properties of materials may be cited: André et al. [15] proposed an experimental system based on the hot-wire method; Jannot et al. [16, 17] developed a tiny hot-plate method for the thermal conductivity measurement of heterogeneous materials [18].

Nevertheless, for non-homogeneous components and for structures composed of different materials (doors, windows, etc.), other techniques are used, and the most common one for the thermal transmittance evaluation is the Hot-Box [19–21], in compliance with the standards EN ISO 8990 [22] and EN ISO 12567-1 [23]. In particular, EN ISO 12567-1 specifies a method to measure the thermal transmittance of doors or windows (the rate of heat flow through the unit area of a building component divided by the temperature difference between both sides of the component). The sample is positioned between two rooms maintained at different temperatures in steady-state conditions (the so-called hot and the cold chambers). The external envelopes of the apparatus have to be well insulated, in order to minimize conduction losses and the heat flux through the walls. The thermal resistance of the specimen could be obtained by measuring the power required to keep the hot chamber at constant temperature and the temperature difference between the hot and the cold chambers (Hot-Box Method, HBM). Preliminary calibration measurements have to be carried out in order to evaluate the heat losses, such as heat transfer through the surround panel and all flanking losses.

At the Department of Engineering of the University of Perugia, according to UNI EN ISO 8990 [22], a Calibrated Hot-Box was built [24–28]. The external walls of the apparatus is composed of a panel of wood and a layer of expanded polystyrene (λ equal to $0.034 \text{ W} \cdot (\text{m}^{-1} \cdot \text{K}^{-1})$), for a total thermal transmittance of about $0.134 \text{ W} \cdot (\text{m}^{-2} \cdot \text{K}^{-1})$. The apparatus is positioned in a laboratory at fixed temperature. The surface temperatures of the samples are measured by 64 thermocouples (copper/constantan junction): 38 in the cold room and 26 in the hot room.

The temperatures of the two chambers are maintained constant: a heating system for the hot room and a cooling system for the cold one are installed to this end. Two ventilation systems are placed in both the chambers, in order to avoid air thermal stratification [27, 28].

Non-homogeneous materials, windows and doors can be installed in order to evaluate their thermal transmittance. For windows overall surface of which is lower than 2.3 m^2 , the sample dimensions are equal to $1.23 \text{ m} \times 1.48 \text{ m}$. The perimeter joints between the surround panel and the specimen shall be sealed on both the sides with tape, caulking or mastic material.

Other experimental apparatuses could be used in order to test homogeneous components as, for example, the guarded hot-plate or the heat-flow meter system (EN ISO 12667 and ASTM C518–10 [29,30]). The heat-flow meter apparatus is a comparative device that uses a reference material with known thermal properties for the system calibration. It is able to establish steady-state one-dimensional heat flux through a test specimen between two parallel plates, at constant, although different temperatures. Fourier's law of heat conduction is used to calculate thermal conductivity and thermal resistivity, or thermal resistance and thermal conductance. A square sample with a thickness up to 10 cm can be placed between two flat plates that are controlled to a specified constant temperature. Thermocouples fixed in the plates surfaces measure the temperature drop across the specimen, and wireless thermal flux meters (HFMs), embedded in each plate, measure the heat flow through the specimen. Thermal flux meters are usually located in the centre of the plates. The guarded area ensures a one-dimensional heat transfer through the measuring area when a homogeneous sample is tested [31]. The thermal conductivity of the specimen (λ in $\text{W}\cdot(\text{m}^{-1}\cdot\text{K}^{-1})$) in steady state can be calculated by means of the heat flux (q_{sp} in $\text{W}\cdot\text{m}^{-2}$), the temperature difference across the specimen (ΔT_{sm} in K) and the thickness of the specimen (s in m).

In the present paper, a new experimental measurement apparatus, named Small Hot-Box, is proposed: the experimental system has been designed and built at the Laboratory of Building Physics, University of Perugia, and preliminary calibration measurements were carried out. The new apparatus allows the thermal conductivity evaluation of homogeneous small samples (300 mm \times 300 mm), the principle of operation of which arises from the Hot-Box method. In comparison with the standard Hot-Box apparatus, the most important advantage of this system is the possibility of testing smaller homogeneous materials in a smaller device. Moreover, it can provide a thermal transmittance value measured in conditions similar to the *in-situ* ones: this is not possible by means of the Hot-Plate apparatus. No standards are available for this original system, and the mode of operation is in developing stage. In the present paper, the description of the apparatus, the working principles and the preliminary calibration measurements are presented. Different kinds of materials were selected for the experimental campaigns (insulation systems, cement blocks, plasterboard, and wood). Two alternative methodologies are described: the thermal flux meter method and the Hot-Box one, and a first comparison between the two methods is exposed. Considering the Hot-Box method, two options of calibration were evaluated: the first one considered only one calibration curve, the second option took into account three curves, considering different ranges of thermal conductivity.

The operation of this original apparatus could be further improved by modifying the original project and by testing other samples in different thermal conductivity ranges.

2 Materials and Methods: The Small Hot-Box Setup

2.1 Construction and Development of the Apparatus

A new experimental apparatus was designed and built at the Laboratory of Building Physics at the University of Perugia for the evaluation of the thermal conductivity of

building homogeneous materials; no reference standards are available for this specific system.

The experimental setup is composed of one box with external dimensions of 0.94 m × 0.50 m × 0.94 m high: it represents the hot side. In order to reduce the heat losses through the structure, the perimeter walls of the chamber have a very thick insulation layer (200 mm of foam polyurethane + 20 mm of wood). The thermal conductivity λ of the polyurethane is $0.0245 \text{ W}\cdot\text{m}^{-1}\cdot\text{K}^{-1}$ for a total thermal transmittance of the walls equal to $0.114 \text{ W}\cdot\text{m}^{-2}\cdot\text{K}^{-1}$ (the thermal conductivity was measured by means of a heat flow meter apparatus [32], at a reference temperature of 20 °C, with an accuracy of $\pm 2 \%$). The total thermal transmittance of the wall was calculated by means of Eq. 1:

$$H = \frac{1}{\left(R_{Si} + \frac{s_{wo}}{\lambda_{wo}} + \frac{s_{pol}}{\lambda_{pol}} + \frac{s_{wo}}{\lambda_{wo}} + R_{Se} \right)} [\text{W}\cdot\text{m}^{-2}\cdot\text{K}^{-1}] \quad (1)$$

where R_{Si} is the internal surface thermal resistance ($\text{m}^2\cdot\text{K}\cdot\text{W}^{-1}$)—it was considered equal to $0.13 \text{ (m}^2\cdot\text{K}\cdot\text{W}^{-1})$ [33] that is the indoor surface resistance of air layers that skims a vertical wall (horizontal direction of the heat flow); R_{Se} is the external surface thermal resistance ($\text{m}^2\cdot\text{K}\cdot\text{W}^{-1}$)—it was considered equal to $0.13 \text{ (m}^2\cdot\text{K}\cdot\text{W}^{-1})$ [33] that is the indoor surface resistance of air layers that skims a vertical wall (horizontal direction of the heat flow); s_{pol} is the thickness of the expanded polyurethane panel (m); s_{wo} is the thickness of the wood panel (m); λ_{pol} thermal conductivity of the expanded polyurethane panel ($\text{W}\cdot\text{m}^{-1}\cdot\text{K}^{-1}$); λ_{wo} is the thermal conductivity of the wood panel ($\text{W}\cdot\text{m}^{-1}\cdot\text{K}^{-1}$). R_{Si} and R_{Se} are both equal to $0.13 \text{ (m}^2\cdot\text{K})\cdot\text{W}^{-1}$, because also the external side (cold room) is indoor (natural convection conditions).

Also the closure side of the box (dimensions 0.94 m × 0.94 m × 0.20 m thick) has a sandwich structure composed of two panels of wood (20 mm each) with a middle layer of expanded polyurethane (200 mm). In the central part of the closure wall, there is an opening for the placement of the sample: the specimens to be examined are square panels with 0.30 m × 0.30 m external dimensions. The edges (contact zones between the support panel and the sample) are covered with insulation rubber. The joints are also sealed with silicone in order to avoid perimeter losses.

The cold side of the apparatus is a small room (3.39 m × 4.22 m × 3 m high) completely insulated from the outside. The new apparatus is positioned inside this ambient, where the general HVAC system of the room permits to maintain a constant temperature. It was monitored during a long period before the construction of the apparatus in different positions near the system, and it was observed that the daily temperatures are rather steady (maximum difference of about 0.8 °C, see Fig. 1). Furthermore the test periods were chosen in a range with a maximum variation of the air temperature of about 0.2 °C to 0.3 °C. This period (generally about 2 h to 3 h) could be considered long enough because many preliminary tests were carried out for each specimens also selecting longer periods (4 h to 5 h), and it was observed that the final value of the measured thermal conductivity was the same considering a longer period. Each time, the test duration should be modified considering the type of the

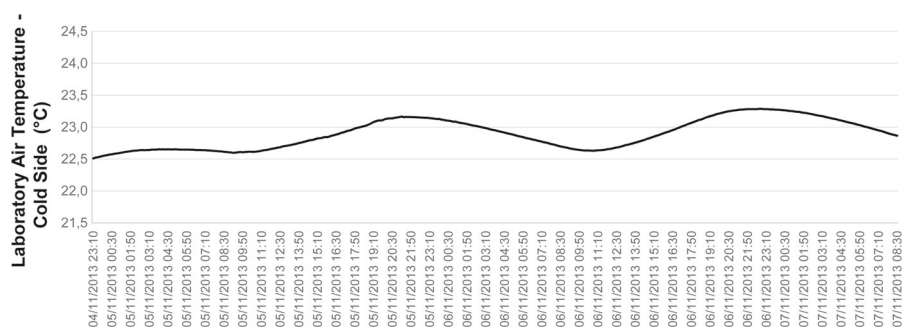


Fig. 1 Typical trend of the Laboratory air temperature (cold side) during 2 days

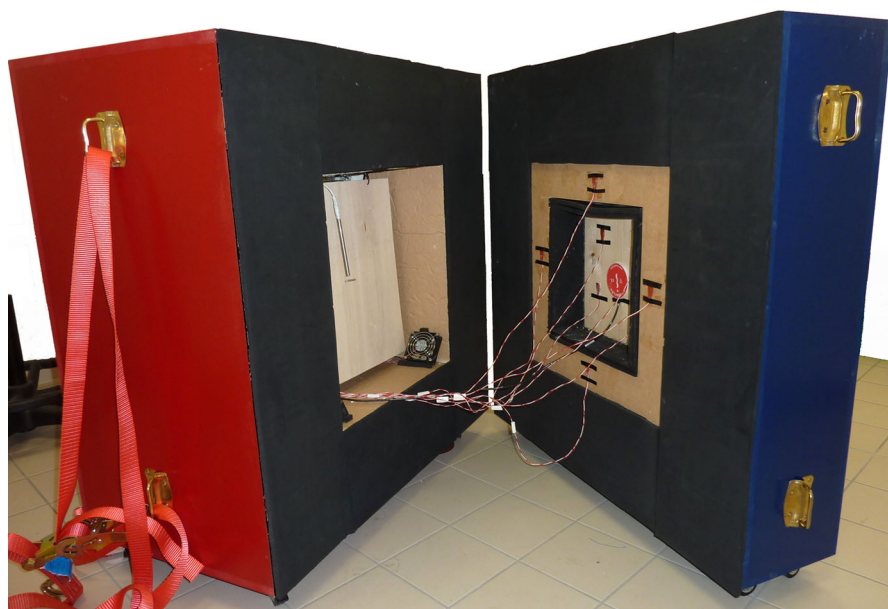


Fig. 2 General view of the apparatus Small Hot-Box

sample and its thickness. The measurement duration should be selected after many preliminary tests.

Both the parts of the Hot-Box system are provided with wheels for their movement, while two strap belts are used for the closure of the apparatus.

A ‘S-shaped’ heating wire 3 m long with a power of 50 W is installed inside the hot room for the regulation of the temperature: it can switch on and off automatically. It is placed in the bottom side of the box; a wooden screen (named *baffle*) is positioned between the heating source and the support panel in order to avoid direct radiations. The emissivity of the screen should be preferably higher than 0.80, so a poplar wood panel with an emissivity of around 0.90, was chosen.

A general view of the apparatus is shown in Fig. 2, while an enlarged exploded view drawing is sketched in Fig. 3. Inside the box, four resistance thermometers are

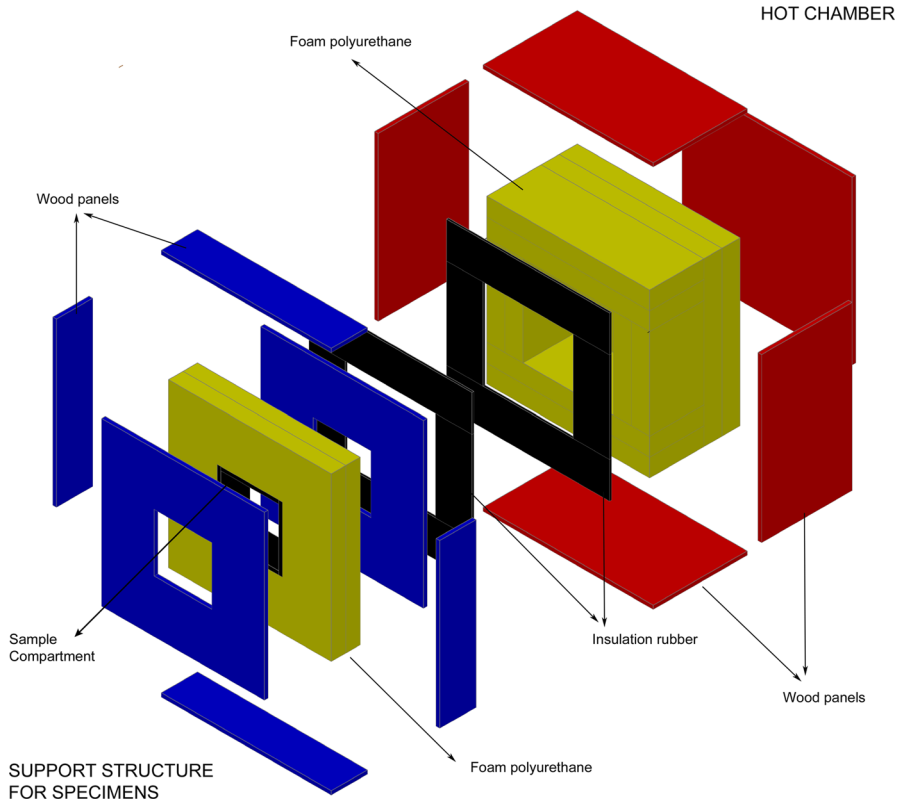


Fig. 3 Exploded 3D view of the apparatus

installed for the control of the surface temperature of the panel in the hot side; four probes are also placed on the support panel surface, and one resistance thermometer monitors the inside air temperature. In the cold room (laboratory), eight probes are fixed to the surfaces in the same correspondent positions of the hot side, and other two resistance thermometers are placed in the room for the air-temperature monitoring of the cold side. For the evaluation of the heat flux from the hot side to the cold one, a thermal flux meter is placed in the central area of the sample. The apparatus with the sensors' positions is represented in Fig. 4; the accuracies of the probes are reported in Table 1. All the monitored data could be transferred to a PC for the management of all the parameters and the data storage.

In preliminary experimental campaigns, the surface temperatures in the hot side showed a difference of about $2\text{ }^{\circ}\text{C}$ to $3\text{ }^{\circ}\text{C}$ between top and bottom of the sample, showing a stratification in the air. Two fans (each one with an electric current equal to 0.11 A) were therefore installed inside the hot chamber: a convective equilibrium was achieved thanks to this ventilation system, and a maximum difference of about $0.6\text{ }^{\circ}\text{C}$ on the hot face was achieved after the fans' installation. At the beginning, the speed value was maintained constant, and the input power attributed to the fans was considered equal to 2.2 W . At the cold side, the air temperatures observed during the

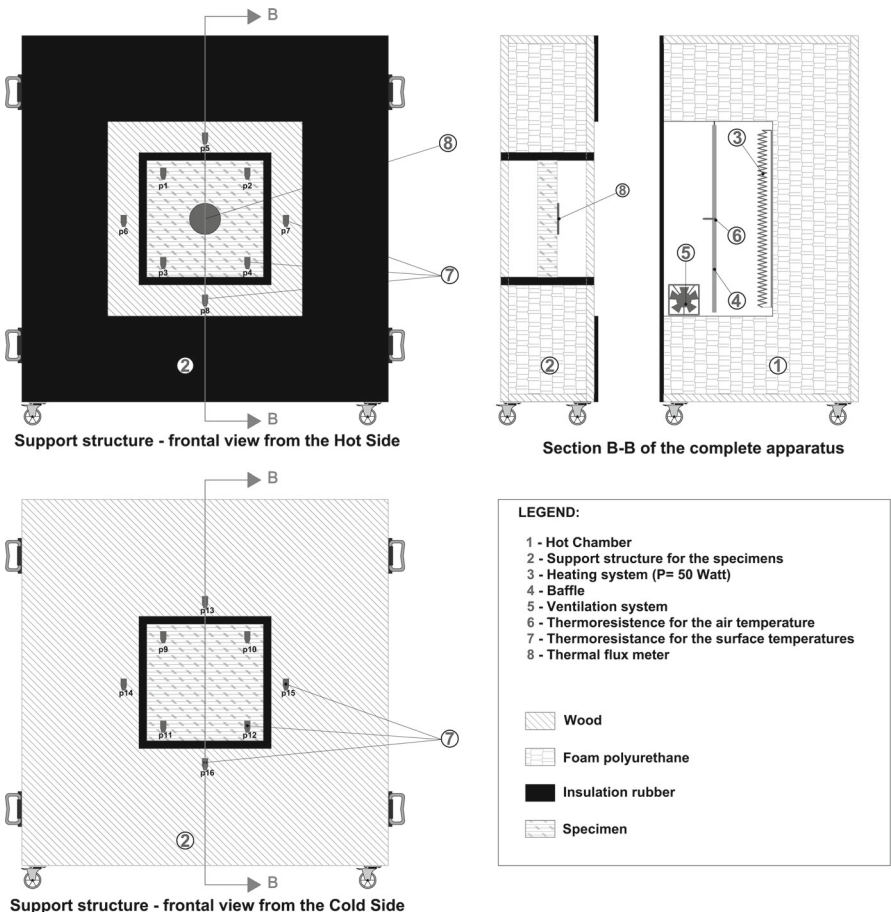


Fig. 4 Apparatus diagrams and sensors' positions

Table 1 Characteristics and accuracy levels of the probes

Probes	Characteristics and accuracy
N.17 thermal resistances for surface and air-temperature measurement	Measurement element: PT100 (platinum resistance thermometers) Measurement range: -200°C to $+800^{\circ}\text{C}$ Accuracy: $\pm 0.05\%$
N.1 Thermal flux meter (diameter 80 mm)	Measurement element: passive thermopile type Measurement range: $-2000\text{ W}\cdot\text{m}^{-2}$ to $+2000\text{ W}\cdot\text{m}^{-2}$ Expected typical accuracy: $\pm 5\%$ Nominal sensitivity: $50\text{ }\mu\text{V}\cdot\text{W}^{-1}\cdot\text{m}^{-2}$

preliminary tests were rather constant and uniform (the air temperature was monitored in different positions). Also the surface temperatures of the cold face were constant with maximum differences in 0.3°C to 0.5°C range.

A switchboard composed of a master switch, a PID controller, an electrical energy meter and a speed variator for the regulation of the fans' velocity was assembled. An ammeter was also installed for the measurement of the current through the hot wire and then for the evaluation of the power supplied to the box in order to keep the steady-state conditions. The electric energy meter measures the energy entering the hot side; this energy can also be calculated as the product of the hot-wire thermal resistance (measured in Ohm) and the square of the current through the hot wire (in Ampere).

2.2 Selection of the Samples for Calibration

In order to calibrate the new experimental apparatus, different samples with known thermal properties were analysed. In particular, three types of insulation specimens: a wood panel, a plasterboard panel and two insulating cement blocks were considered, for a total number of seven samples. The thermal conductivities of the selected samples are certified by the manufacturers, so the measured values were compared with the declared ones (all the declared values were measured in other labs by means of Heat Flow Meter method (EN ISO 12667)). The main characteristics of the samples are reported in Table 2 (thickness, thermal conductivity, and number of tests carried out). The experimental campaigns were carried out during the periods of June–September 2014 and March–May 2015. The thermal conductivity was evaluated by means of both the thermal flux meter methodology and the Hot-Box one. The hot chamber set-point temperatures were not the same for all the tested materials, and they were chosen considering the laboratory air temperatures during the test; an air temperature difference of at least 20 °C was in fact maintained between the hot and the cold side. When the mean air temperature of the cold chamber was high (about 30 °C), the set-point air temperature of the hot side was imposed equal to 55 °C, whereas when the laboratory air temperature was lower (about 20 °C), it was imposed equal to 45 °C. More specimens of the same type were tested but, generally, the differences of the final measured thermal conductivities are less than 2 %.

3 Results and Discussion

3.1 Thermal Flux Meter Method

A thermal flux meter is installed in the central part of the sample, as shown in Fig. 4. The probe (HFP01—Hukseflux) is a thermopile operating in the $-2000 \text{ W}\cdot\text{m}^{-2}$ to $+2000 \text{ W}\cdot\text{m}^{-2}$ power range and in the $-30 \text{ }^{\circ}\text{C}$ to $+70 \text{ }^{\circ}\text{C}$ temperature range. The thermopile generates a small output voltage proportional to the local heat flux. As already mentioned, for the thermal conductivity calculation, four resistance thermometers on each side are installed on the hot and cold surfaces of the sample (Fig. 4). The thermal resistance R_t could be calculated as follows (Progressive Average Methodology) [37,38]:

Table 2 Main description of the tested samples






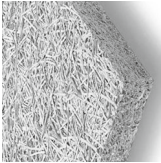

Sample	s (mm)	λ declared ($\text{W}\cdot\text{m}^{-1}\cdot\text{K}^{-1}$)	Absolute thermal conductivity accuracy (%)	Picture	Test	Set-point temperature (Hot Room) ($^{\circ}\text{C}$)
A) Foam polyurethane	100	0.0245 (at a reference temperature of 20 $^{\circ}\text{C}$) [32]	$\pm 2\%$ [32]		A1 A2	50 55
B) Polystyrol	60	0.0350 (at a reference temperature of 20 $^{\circ}\text{C}$) [32]	$\pm 2\%$ [32]		B1 B2	45 50
C) Polystyrene	50	0.0370 (at a reference temperature of 20 $^{\circ}\text{C}$) [32]	$\pm 2\%$ [32]		C1 C2	45 50
D) Wood	50	0.120 (at a reference temperature of 20 $^{\circ}\text{C}$) [32]	$\pm 2\%$ [32]		D1 D2	45 50

Table 2 continued

Sample	s (mm)	λ declared ($\text{W}\cdot\text{m}^{-1}\cdot\text{K}^{-1}$)	Absolute thermal conductivity accuracy (%)	Picture	Test	Set-point temperature (Hot Room) ($^{\circ}\text{C}$)
E) Plasterboard	40	0.200 (at a reference temperature of 20°C) [33]	$\pm 2\%$ [34]		E1 E2	45 50
F) Cement block+mineral fibers	72	0.065 (at a reference temperature of 20°C) [35]	Not available		F1 F2	45 50
G) Cement block with sand and additives	100	0.045 (at a reference temperature of 20°C) [36]	Not available		G1 G2	45 50

$$R_t = \frac{\sum_{j=1}^n (T_{pHj} - T_{pCj})}{\sum_{j=1}^n q_j} \left[(\text{m}^2 \cdot \text{K}) \cdot \text{W}^{-1} \right] \quad (2)$$

where the index j is related to each acquisition time.

The thermal conductivity can be calculated by the mean value of the thermal resistance R_t during the selected period (about 2 h to 3 h) and the thickness of the specimen (s in m) as follows:

$$\lambda = s / R_t \left[\text{W} \cdot (\text{m}^{-1} \cdot \text{K}^{-1}) \right] \quad (3)$$

The experimental results of the thermal flux meter measurements for the sample A are reported in Fig. 5 considering a set point temperature of 50 °C (test A1). The test was carried out on June 11th, and it lasted for about 3 h. All the surface temperatures were constant during the test, with a maximum difference of about 0.6 °C on the hot face and 0.4 °C on the cold one. The air-temperature trend was constant in the hot chamber (about ± 0.1 °C); in the laboratory (cold side) the air temperature's maximum difference is about 0.3 °C (Fig. 5). This variation seems to be acceptable considering that the fluctuation should not exceed the 1 % of the air temperature differences between the cold and hot sides (EN ISO 8990: Thermal insulation—Determination of steady state thermal transmission properties—Calibrated and guarded Hot-Box) (ΔT_{air} is equal to 28.6 °C for this test and generally $\Delta T_{\text{air}} > 20$ °C for all the tests). The reference mean air temperature observed during each test is also shown in Table 3 (it is the average between the mean air temperatures measured in the hot side and the mean values measured in the cold one during the test).

It can be observed that the thermal resistance trend was quite stable because a selected period with a constant value of the air temperature in both the chamber was chosen; R_t converged to the value of $3.94 \text{ m}^2 \cdot \text{K} \cdot \text{W}^{-1}$; the corresponding thermal conductivity value is $0.0254 \text{ W} \cdot \text{m}^{-1} \cdot \text{K}^{-1}$, with an error of about +3.6 % (the declared value is $0.0245 \text{ W} \cdot \text{m}^{-1} \cdot \text{K}^{-1}$, certified according to UNI EN ISO 12667).

The final values of the thermal conductivity obtained for the other samples are reported in Table 3, compared with the declared values. A mean error of about 10 % was found when considering the different samples and in different test conditions.

3.2 Hot-Box method

The Hot-Box method allows the evaluation of the heat flux through the sample as the difference between the input power (P_i in W) in the hot chamber and the heat losses through the walls and the thermal bridges (P_w in W). The losses, represented by the term P_w , are evaluated by means of calibration measurements. P_w shall be plotted vs. the air-temperature difference between the hot and the cold sides.

A specific calibration panel was assembled for the preliminary calibration tests, and many measurements were carried out by considering different set-point temperatures of the hot chamber (the air-temperature difference between hot and cold side was maintained higher than 20 °C for all the tests). Two different attempts were considered: in the first calibration procedure, the measurements were carried out only with the assembled calibration panel (Sect. 3.2.1); in the second one, the measurements on

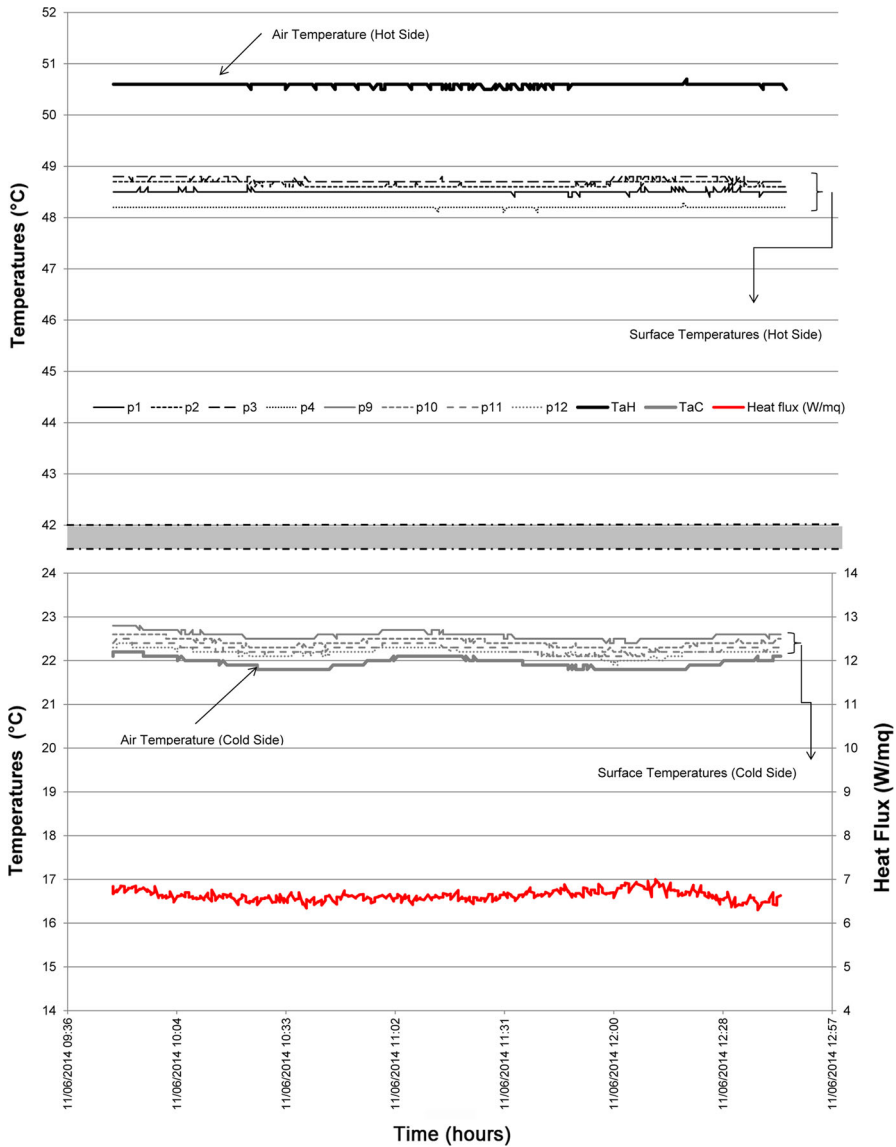


Fig. 5 Test A1-Measured air temperatures, surface temperatures and heat fluxes in the hot and cold chambers

different specimens with known thermal properties (see Table 2) were used for the construction of the calibration curves (Sect. 3.2.2).

3.2.1 Preliminary Calibration Measurements

The heat flux through the walls of the apparatus was evaluated considering the difference between the input heat flux (due to the hot wire and the fans) and the heat flux

Table 3 Thermal conductivity values and percentage errors with thermal flux meter method and Hot-Box method (preliminary calibration)

Sample	Set-point temp. for each test (Hot Room) (°C)	Air temp. difference ΔT_a (°C)	Reference mean air temp. during the test $T_{a,m}$ (°C)	Mean surf. temp. of samples $T_{s,m}$ (°C)	$\lambda_{declared}$ ($W \cdot m^{-1} \cdot K^{-1}$)	Thermal flux meter method λ_{tfm} ($W \cdot m^{-1} \cdot K^{-1}$)	e (%)	Hot-box method λ_{HB} ($W \cdot m^{-1} \cdot K^{-1}$)	e (%)
A) Foam polyurethane	A1 50	28.6	36.3	35.4	0.0245	0.0254	+3.6	0.0379	+54.6
B) Polystyrol	A2 55	33.4	38.8	38.0		0.0259	+5.7	0.0393	+60.5
	B1 45	20.1	35.7	34.7	0.035	0.039	+11.4	0.0403	+15.2
	B2 50	24.9	38.3	37.3		0.040	+14.3	0.0395	+13.0
	C1 45	20.6	35.9	34.8	0.037	0.041	+10.8	0.0406	+9.7
C) Polystyrene	C2 50	26.0	37.6	36.8		0.043	+16.2	0.0326	-12.0
	D1 45	21.7	34.8	34.1	0.120	0.104	-13.3	0.1516	+26.3
	D2 50	26.2	37.6	37.0		0.105	-12.5	0.1124	-6.4
	E1 45	27.1	36.7	36.2	0.200	0.190	-5.0	0.2159	+8.0
E) Plasterboard	E2 50	29.6	35.4	35.1		0.189	-5.5	0.1757	-12.2
	F1 45	22.8	34.1	32.8	0.065	0.075	+15.3	0.0728	+12.0
F) Cement block+mineral fibers	F2 50	28.0	35.9	34.5		0.080	+23.0	0.0926	+42.5
G) Cement block with sand and additives	G1 45	22.8	33.7	32.3	0.045	0.0449	-0.2	0.0508	+12.9
	G2 50	27.2	34.1	32.6		0.0448	-0.4	0.0633	+40.7
					Mean error (%)	Mean error (%)	9.8		23.2

through the panel (known because the calibration panel properties are known). The panel is composed by three layers: an expanded polyurethane panel 0.06 m thick (s_{pol}), covered on the external surfaces by two sheets of tempered float glass, 0.004 m thick (s_g). The thermal conductivity of polyurethane λ_{pol} is equal to $0.034 \text{ W}\cdot\text{m}^{-1}\cdot\text{K}^{-1}$, and the thermal conductivity of the glazing layer λ_g is equal to $1 \text{ W}\cdot\text{m}^{-1}\cdot\text{K}^{-1}$ (supplied by the manufacturer); therefore, the total value of the thermal conductance C of the panel ($s_t = 68 \text{ mm}$) is about $0.564 \text{ W}\cdot\text{m}^{-2}\cdot\text{K}^{-1}$, and the equivalent thermal conductivity is $0.038 \text{ W}\cdot\text{m}^{-1}\cdot\text{K}^{-1}$.

The thermal conductance of the total specimen was evaluated as follows:

$$C = \frac{1}{\left(\frac{s_g}{\lambda_g} + \frac{s_{pol}}{\lambda_{pol}} + \frac{s_g}{\lambda_g}\right)} \left[\text{W}\cdot\text{m}^{-2}\cdot\text{K}^{-1} \right] \quad (4)$$

and the equivalent thermal conductivity is consequently calculated as

$$\lambda_{eq} = C \cdot s_t \left[\text{W}\cdot\text{m}^{-1}\cdot\text{K}^{-1} \right] \quad (5)$$

The calibration of the panel was carried out several times; in this paper, only the last calibration results are reported. However, the calibration will be periodically checked. The heat fluxes through the walls and through thermal bridges P_w were calculated as the difference between the input power in the hot chamber P_i and the heat flux through the calibration panel P_p : $P_w = P_i - P_p$.

The incoming power P_i can be measured considering two contributions: the heat flux released by the resistance during the test (P_r in W) and the contribution of the fans (P_f in W). The thermal power transferred from the hot chamber to the cold side through the calibration sample (P_p in W) can be evaluated as the product of the thermal conductance of the panel (C in $\text{W}\cdot\text{m}^{-2}\cdot\text{K}^{-1}$), known the surface of the panel (A in m^2), and the difference of the surface temperatures (hot and cold sides) (see Eq. 6):

$$P_p = C \cdot A \cdot (T_{pH} - T_{pC}) \quad [\text{W}] \quad (6)$$

Considering this configuration, four tests were carried out by modifying the temperature in the hot room (45°C , 50°C , 55°C , and 60°C). The cold room temperatures were not modified in the four cases, but during the tests a constant value was observed (about 22°C). The experimental campaign was completed during the period of May–June 2014. The main results of the experimental tests are reported in Table 4. The linear regression is the following:

$$P_w = 0.2062 \cdot (T_{aH} - T_{aC}) + 2.2925 \quad [\text{W}] \quad (7)$$

The regression line coefficient is equal to 0.9391. The calibration curve is represented in Fig. 6, and it was applied to the preliminary tests carried out on the samples in Table 2 for calculating the thermal conductivity by means of the Hot-Box method. The power coming out through the tested specimens (P_s in W) was evaluated as the difference between the measured entering power in the hot chamber (P_i in W) and the value

Table 4 Preliminary calibration measurements results

Set-point temperature (Hot Room) (°C)	ΔT_{air} (°C)	Mean air temperatures of rooms $T_{a,m}$ (°C)	ΔT_S (°C)	Mean surf. temperatures of samples $T_{s,m}$ (°C)	P_i (W)	P_p (W)	P_w (W)
45	22.78	34.2	19.40	32.9	7.76	1.02	6.74
50	28.00	36.6	23.89	35.4	9.51	1.25	8.26
55	32.76	39.2	27.93	37.9	10.88	1.46	9.42
60	37.61	41.8	31.87	40.4	11.4	1.67	9.73

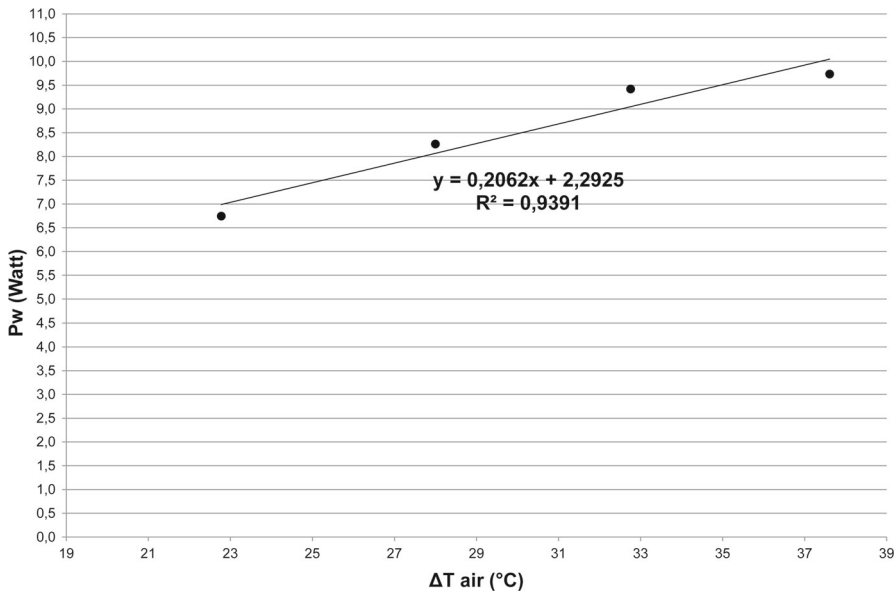


Fig. 6 Preliminary calibration curve's trend considering the experimental measurements carried out with the calibration panel

P_w evaluated from the calibration curve's equation (Eq. 7), known the temperature difference between hot and cold sides:

$$P_s = P_i - P_w \quad [\text{W}] \quad (8)$$

The thermal conductivity of the specimen is determined by dividing the power through the specimen (P_s in W) by the area of the specimen A_s (m^2) and the temperature difference of the two surfaces: ($T_{sH} - T_{sC}$, where T_{sH} is the surface temperature of the sample in the hot side, and T_{sC} is the surface temperature of the sample in the cold one):

$$\lambda = \frac{P_s \cdot s}{A_s \cdot (T_{sH} - T_{sC})} \left[\text{W} \cdot (\text{m}^{-1} \cdot \text{K}^{-1}) \right] \quad (9)$$

The results are reported in Table 3, in comparison with the real values (certified by the producers). The percentage error is included in 10 % to 15 % range when considering the specimens with a thermal conductivity comparable with the calibration panel (samples B and C, $0.035 \text{ W} \cdot \text{m}^{-1} \cdot \text{K}^{-1}$ to $0.037 \text{ W} \cdot \text{m}^{-1} \cdot \text{K}^{-1}$), while for the foam polyurethane (sample A), it is about 50 % to 60 % ($\lambda = 0.0245 \text{ W} \cdot \text{m}^{-1} \cdot \text{K}^{-1}$); therefore, the calibration curve (7) could not be applied for this specimen. The same happens also for the cement block type F, when the mean error exceeds 30 %. In general, the thermal conductivity is overestimated for most of the samples. For wood (sample D) and plasterboard (sample E), the curve could not seem to be appropriate because their thermal conductivity values are much too high (0.12 and 0.20 , respectively: $\text{W} \cdot \text{m}^{-1} \cdot \text{K}^{-1}$) with respect to the one of the calibration panel, but the error percentage is not too much

high (−6 % to 26 %). Furthermore for wood, plasterboard and polystyrene, the thermal conductivities are underestimated, considering the test with an air temperature of the hot side fixed to 50 °C. Finally, for almost all the measurements, the results are better considering a fixed hot-side temperature equal to 45 °C. In conclusion, it seems to be incorrect to consider only this calibration curve.

3.2.2 Calibration of the Apparatus

After the first calibration, a second method was considered: different calibration curves were traced for different thermal conductivity ranges. The methodology for the calibration curves achievement is the same as the one used for the preliminary calibration curve (Eq. 7), and it is described in Sect. 3.2.1. Each curve is the linear regression obtained from the punctual values of the P_w (in W, heat flux through the walls and the thermal bridges) versus the corresponding measured mean air-temperature differences between the hot and cold sides. In the future, many other tests have to be carried out in order to make the calibration curves more definite. In Fig. 7, a preliminary draft of the results of this approach is represented, considering the first experimental campaign described in the present paper; three curves are reported: the first one for the thermal conductivity range $0.02 \text{ W}\cdot\text{m}^{-1}\cdot\text{K}^{-1}$ to $0.05 \text{ W}\cdot\text{m}^{-1}\cdot\text{K}^{-1}$, the second one for higher thermal conductivities ($>0.05 \text{ W}\cdot\text{m}^{-1}\cdot\text{K}^{-1}$) and the last one considering all the tested materials. The first curve (*Calibration curve n.1*) was obtained by using the tests on the specimens: A, B, C and G (λ in the $0.0245 \text{ W}\cdot\text{m}^{-1}\cdot\text{K}^{-1}$ to $0.045 \text{ W}\cdot\text{m}^{-1}\cdot\text{K}^{-1}$ range). The curve was traced considering the measurements singularly carried out for the specimens A, B, C and G: the linear regression curve is obtained from the points represented

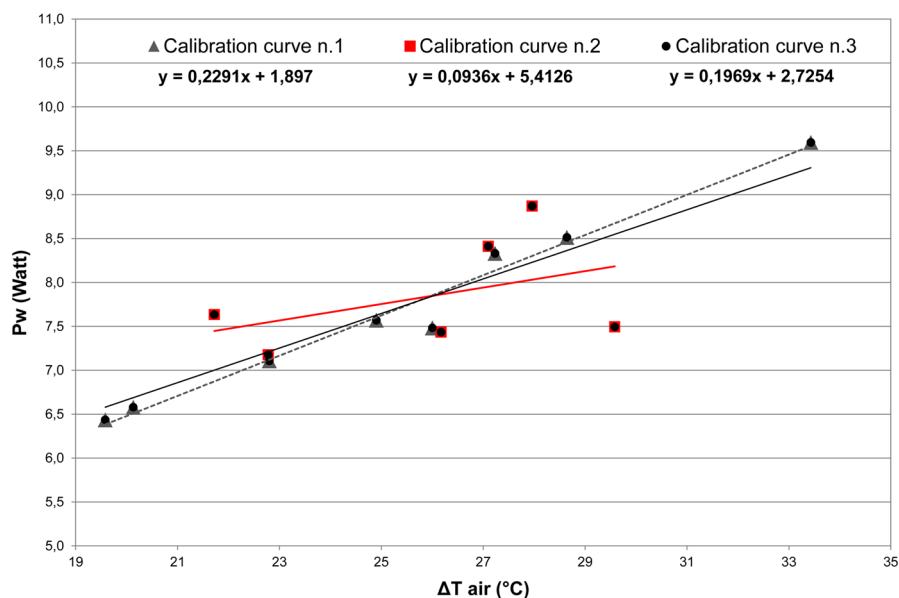


Fig. 7 Preliminary draft of three calibration curves considering different ranges of thermal conductivity

Table 5 Thermal conductivity values and percentage errors with Hot-Box method considering new calibration curves (n.1,2 and 3)

Sample	Set-point temp. for each test (Hot Room) (°C)	Air temp. difference ΔT_a (°C)	Reference mean air temp. during the test $T_{a,m}$ (°C)	Mean surf. temp. of sample $T_{s,m}$ (°C)	$\lambda_{declared}$ (W·m ⁻¹ ·K ⁻¹)	Hot-Box Method <i>Calib. curve n.1</i> λ_{HB} (W·m ⁻¹ ·K ⁻¹)	e (%)	Hot-Box Method <i>Calib. curve n.2</i> λ_{HB} (W·m ⁻¹ ·K ⁻¹)	e (%)	Hot-Box Method <i>Calib. curve n.3</i> λ_{HB} (W·m ⁻¹ ·K ⁻¹)	e (%)
A) Foam polyurethane	A1 50	28.6	36.3	35.4	0.0245	0.0268	+9.5	-	-	0.0308	+25.8
	A2 55	33.4	38.8	38.0		0.0259	+5.7	-	-	0.0349	+42.4
B) Polystyrol	B1 45	20.1	35.7	34.7	0.035	0.0378	+7.9	-	-	0.0307	-12.3
	B2 50	24.9	38.3	37.3		0.0340	-2.8	-	-	0.0332	-5.2
C) Polystyrene	C1 45	20.6	35.9	34.8	0.037	0.0388	+4.8	-	-	0.0320	-13.4
	C2 50	26.0	37.6	36.8		0.0274	-26.0	-	-	0.0276	-25.4
D) Wood	D1 45	21.7	34.8	34.1	0.120	-	-	0.1269	+5.7	0.1431	+19.3
	D2 50	26.2	37.6	37.0		-	-	0.1071	-10.7	0.1066	-11.1
E) Plasterboard	E1 45	27.1	36.7	36.2	0.200	-	-	0.2138	+6.9	0.2105	+5.2
	E2 50	29.6	35.4	35.1		-	-	0.1814	-9.3	0.1714	-14.3
F) Cement block+mineral fibers	F1 45	22.8	34.1	32.8	0.065	-	-	0.0497	-23.5	0.0636	-2.2
	F2 50	28.0	35.9	34.5		-	-	0.0936	+44.0	0.0867	+33.5
G) Cement block with sand and additives	G1 45	22.8	33.7	32.3	0.045	0.0443	-1.6	-	-	0.0394	-12.4
	G2 50	27.2	34.1	32.6		0.0535	+18.8	-	-	0.0556	+23.5
Mean error (%)							9.6	Mean error (%)	16.7	Mean error (%)	17.5

in Fig. 7 (P_w vs. $\Delta T_{air} = (T_{aH} - T_{aC})$) obtained for the singular measurement—the measurements for different set-point temperatures are the ones shown in Table 3). The second curve (*Calibration curve n.2*) was obtained from the tests carried out with the specimens: F ($\lambda = 0.065 \text{ W}\cdot\text{m}^{-1}\cdot\text{K}^{-1}$), D ($\lambda = 0.12 \text{ W}\cdot\text{m}^{-1}\cdot\text{K}^{-1}$) and E ($\lambda = 0.20 \text{ W}\cdot\text{m}^{-1}\cdot\text{K}^{-1}$), and the last one, *Calibration curve n.3*, was found from all the measurements carried out for the seven samples. The curves have to be improved making other experimental analysis by testing different specimens with a thermal conductivities of the same order of magnitude. The aforementioned curves were applied again to the same precious tests, and the results are represented in Table 5. It can be observed that the mean global error is decreased considering the application of the calibration curves 1, 2 and 3 (9.6 % to 17.5 %), with respect to the application of the curve obtained by only the calibration panel. The calibration curve n.1 was adopted for samples with a thermal conductivity values smaller than $0.05 \text{ W}\cdot\text{m}^{-1}\cdot\text{K}^{-1}$. Thanks to the application of this curve, the percentage errors for these materials are decreased from 24.3 % to 9.6 %. The calibration curve n. 2 can be applied to materials with higher thermal conductivities ($>0.05 \text{ W}\cdot\text{m}^{-1}\cdot\text{K}^{-1}$); it can be observed that this curve is suitable for materials with $\lambda > 0.1 \text{ W}\cdot\text{m}^{-1}\cdot\text{K}^{-1}$ such as wood and plasterboard (error values varying in 5 % to 10 % range). Finally, by applying the calibration curve n. 3, the mean error values decrease from 23.2 % to 17.5 %. Nevertheless, it has to be improved by testing many other specimens in order to obtain specific calibration curves for strict ranges of thermal conductivity values. In general, it can be observed that for sample G, the mean error is higher considering the set-point temperature of the hot chamber equal to 50°C , both for calibration curves 1 and 3 (18.8 % and 23.5 % respectively); if the set-point temperature of the hot side is 45°C , mean errors of 1.6 % (calibration curve n.1) and 12.4 % (calibration curve n.3) are obtained. The same behaviour was observed for specimen F, for both calibration curves 2 and 3 (mean errors of 44 % and 33.5 %, respectively). It can be concluded that the absolute value of the mean error increases with the increasing mean air-temperatures difference between hot and the cold sides.

4 Conclusion

The present study highlights the importance of the evaluation of building materials' thermal properties. Thanks to the use of advanced materials with good thermal insulation properties, the heat losses through the building envelope can be significantly reduced [39,40]. In this scenario, an original and novel experimental apparatus was designed and built at the University of Perugia: the Small Hot-Box, as a possible future alternative system to be used instead of the conventional Hot-Plate apparatus for the experimental evaluation of the thermal resistance of homogeneous materials. The most important advantage is that the thickness of the specimens could be higher than the one of Hot-Plate apparatus samples. Moreover, with the Small Hot-Box apparatus, the convective equilibrium in the samples surfaces is comparable to the *in situ* heat transfer. The aim of the project is to try to devise a new system that could be used also for the study of materials with a thermal resistance lower than $0.5 \text{ m}^2\cdot\text{K}\cdot\text{W}^{-1}$.

The apparatus is composed of a hot chamber and a cold side. The air temperatures and the temperatures of the surfaces are measured by means of 16 resistance thermometers and a dedicated acquisition system connected to a PC. The tested samples (dimensions $0.3\text{ m} \times 0.3\text{ m}$) are installed in a support panel between the hot and the cold sides. An air-temperature difference of at least $20\text{ }^{\circ}\text{C}$ is maintained during the test.

Both the thermal flux meter method and the Hot-Box one were considered for the calculation of the thermal conductivity. In the first method, the heat flux through the specimen is directly measured by the thermal flux meter installed on the sample, whereas in the second method, the heat flux is evaluated as the difference between the input heat flux in the metering room and the heat losses through the walls.

In order to evaluate the experimental apparatus mode of operation, different samples with known thermal properties were analysed (polystyrol, foam polyurethane, polystyrene, wood, plasterboard, and cement insulating blocks).

The thermal conductivity values obtained by using the thermal flux meter methodology are higher than the certified values for almost all the specimens, except for the wood, the cement block type G and the plasterboard: in the first case, the thermal conductivity value is lower than $0.12\text{ W}\cdot\text{m}^{-1}\cdot\text{K}^{-1}$ ($0.104\text{ W}\cdot\text{m}^{-1}\cdot\text{K}^{-1}$ to $0.105\text{ W}\cdot\text{m}^{-1}\cdot\text{K}^{-1}$), as for the plasterboard (about $0.18\text{ W}\cdot\text{m}^{-1}\cdot\text{K}^{-1}$ to $0.19\text{ W}\cdot\text{m}^{-1}\cdot\text{K}^{-1}$ instead of $0.20\text{ W}\cdot\text{m}^{-1}\cdot\text{K}^{-1}$). Minimum error values were obtained for tests G1 and G2 (about 0.2 % to 0.4 %) and A1 and A2 (foam polyurethane), with errors being equal to 3.6 % and 5.7 %, respectively. In general, it can be observed that the error increases for higher set-point temperatures of the hot side (from $45\text{ }^{\circ}\text{C}$ to $55\text{ }^{\circ}\text{C}$). The mean value of the error percentage is about 10 % (Table 3).

The Hot-Box method can be applied after a calibration of the apparatus: a preliminary calibration was carried out by means of a calibration panel composed of glass and polystyrene. The thermal conductivity values obtained using the first calibration curve are similar to the declared values only for the samples with comparable thermal conductivities. The calibration curve reported in Eq. 7 was used for the evaluation of the thermal conductivity, and the mean error of about 23.2 % was found (Table 3). In this case, the measured thermal conductivity is higher than the declared value for almost all the samples except for C, D and E, but only when the hot-side air temperature is fixed at $50\text{ }^{\circ}\text{C}$. Furthermore, the thermal conductivity is underestimated, and the Hot-Box methodology with calibration curve (7) can be adopted only for the samples B and C, because they have a thermal conductivity comparable to the one of the calibration panel: ($0.035\text{ W}\cdot\text{m}^{-1}\cdot\text{K}^{-1}$ to $0.037\text{ W}\cdot\text{m}^{-1}\cdot\text{K}^{-1}$). For these samples, the percentage error values vary in 9 % to 15 % range. In the other cases, the errors are higher and not negligible: other calibration curves have to be performed, and a new method was examined in Sect. 3.2.2 (see Fig. 7). Three preliminary calibration curves were constructed in this paper, thanks to experimental campaigns carried out during the periods of spring–summer 2014 and winter–spring 2015. The draft curves took into account the results obtained for the seven samples: curves n. 1 and n. 2 could be used, respectively, for materials with thermal conductivity values $\leq 0.05\text{ W}\cdot\text{m}^{-1}\cdot\text{K}^{-1}$ and higher than $0.05\text{ W}\cdot\text{m}^{-1}\cdot\text{K}^{-1}$ to $0.06\text{ W}\cdot\text{m}^{-1}\cdot\text{K}^{-1}$, with a significant reduction of the mean error (from 23.2 % to about 13 %). It can be observed that the absolute mean error value increases with the increasing the mean air-temperature difference between

the hot and the cold sides. This behaviour was observed for almost all the samples. Hence, the comparison between the declared values (at a reference mean temperature of 20 °C) and the measured λ -values is more significant considering the values obtained for a small set-point air temperature of the hot room equal to 45 °C (mean surface temperatures of about 34 °C to 35 °C). These values can be compared because in both the cases, the mean temperatures of the sides are close to values that could be measured also *in-situ* on the surfaces of the building materials of a wall (considering both winter and summer conditions).

A possible development of the future research should be another experimental campaign considering a value of the set-point temperature of the hot side lower than 45 °C, in order to try to reduce the global mean error. After the study of the measurement uncertainties depending on the mean temperatures, the best mean air-temperature difference will be established. The future development of the Small Hot-Box system will consider the improvement of the Hot-Box methodology: many other materials with known thermal conductivity will be analysed and used for the improvement of calibration curves in different ranges of λ . Furthermore, the system for the evaluation of the input power in the hot chamber will also be improved by installing a voltmeter or a watt-meter. Finally, the research team is planning to assemble a second chamber in order to better control the mean air-temperature of the cold room by fixing an exact set-point temperature also in the cold side.

References

1. E.S. Long, Build. Environ. **40**, 443 (2005)
2. X. Meng, Y. Gao, Y. Wang, B. Yan, W. Zhang, E. Long, Appl. Therm. Eng. **83**, 48 (2015)
3. European Commission, Energy-efficient buildings PPP—multi-annual roadmap and longer term strategy. http://ec.europa.eu/information_society/activities/sustainable_growth/docs/sb_publications/eeb_roadmap.pdf. Accessed 14 Nov 2014
4. C. Buratti, E. Belloni, D. Palladino, Energy Build. **74**, 173 (2014)
5. L. Pérez-Lombard, J. Ortiz, C. Pout, Energy Build. **40**, 394 (2008)
6. BPIE (Building Performance Institute Europe). Europe's Buildings Under the Microscope 2011. http://www.bpie.eu/eu_buildings_under_microscope.html. Accessed 14 Nov 2014
7. Directive 2010/31/EU of the European Parliament and of the Council of 19 May 2010 on the Energy Performance of Buildings (recast)
8. M.J. Assael, K.D. Antoniadis, W.A. Wakeham, Int. J. Thermophys. **31**, 1051 (2010)
9. R. Wulf, G. Barth, U. Gross, Int. J. Thermophys. **28**, 1679 (2007)
10. G. Wei, X. Zhang, F. Yu, J. Univ. Sci. Technol. Beijing Miner. Metall. Mater. **15**, 791 (2008)
11. U. Hammerschmidt, V. Meier, Int. J. Thermophys. **27**, 840 (2006)
12. M.H. Rausch, K. Krzeminski, A. Leipertz, A.P. Fröba, Int. J. Heat Mass Transf. **58**, 610 (2013)
13. G. Salvalai, M. Imperadori, D. Scaccabarozzi, C. Pusceddu, Appl. Therm. Eng. **82**, 110 (2015)
14. American Society for Testing and Materials, *ASTM C177–97: Standard Test Method for Steady-State Heat Flux Measurements and Thermal Transmission Properties by Means of the Guarded-Hot-Plate Apparatus* (West Conshohocken, PA, 1997)
15. S. André, B. Rémy, F. Pereira, N. Cella, Eng. Térm. **4**, 55 (2003)
16. Y. Jannot, V. Felix, A. Degiovanni, Meas. Sci. Technol. **21**, 1 (2010)
17. Y. Jannot, B. Remy, A. Degiovanni, High Temp. High Press. **39**, 11 (2009)
18. N. Laaroussi, G. Lauriat, M. Garoum, A. Cherki, Y. Jannot, Constr. Build. Mater. **70**, 351 (2014)
19. J.R. Mumaw, Calibrated hot box: an effective means for measuring thermal conductance in large wall sections. In: American Society for Testing and Materials, ASTM STP 544, heat transmission measurements in thermal insulations (West Conshohocken, PA, 1974), pp. 193–211

20. J.H. Klems, A calibrated hot box for testing window systems—construction calibration and measurements on prototype high-performance windows, In: Proceedings of ASHRAE/DOE-ORNL Conference on Thermal Performance of the Exterior Envelopes of Buildings (Kissimmee, Florida, 1979), pp. 338–346
21. A. Ghosh, S. Ghosh, S. Neogi. Performance evaluation of a Guarded Hot Box U-value measurement facility under different software based temperature control strategies. in *4th International Conference on Advances in Energy Research 2013, ICAER 2013*. Energy Procedia 54 (2014), pp. 448–454
22. European Standard EN ISO 8990, Thermal insulation—determination of steady-state thermal transmission properties—calibrated and guarded hot box (1996)
23. European Standard EN ISO 12567–1, Thermal performance of windows and doors—determination of thermal transmittance by hot box method—complete windows and doors (2010)
24. C. Fangzhi, K.W. Stephen, Energy Build. **53**, 47–56 (2012)
25. A.H. Elmahdy, K. Haddad, ASHRAE Trans. **106**, 601 (2000)
26. K. Martin, A. Campos-Celador, C. Escudero, I. Gómez, J.M. Sala, Energy Build. **50**, 139 (2012)
27. P. Ricciardi, E. Belloni, F. Cotana, Appl. Energy **134**, 150–162 (2014)
28. F. Asdrubali, G. Baldinelli, Energy Build. **43**, 1618–1626 (2011)
29. European Standard EN ISO 12667, Thermal Performance of Building Materials and Products—Determination of Thermal Resistance by Means of Guarded Hot Plate and Heat Flow Meter Methods—Products of High and Medium Thermal Resistance; ISO: Geneva (2001)
30. American Society for Testing and Materials, ASTM C518–10. Standard Test Method for Steady-State Thermal Transmission Properties by Means of the Heat Flow Meter Apparatus; ASTM: West Conshohocken, PA (2003)
31. S.W. Kim, S.H. Lee, J.S. Kang, K.H. Kang, Int. J. Thermophys. **27**, 1873 (2006)
32. <http://lasercomp.com/product/fox314.php>
33. EN ISO 6946, Building components and building elements—thermal resistance and thermal transmittance—calculation method (2007)
34. <http://www.etermedile.it/Etermedile/files/08/084ee498-007e-4ab8-a7c5-1c76b958ebc6.pdf>, [www.knauf.it/minisitiBase/download/download/030%20-%20Sistema%20Isolamento%20Termico_\(29-1\).pdf](http://www.knauf.it/minisitiBase/download/download/030%20-%20Sistema%20Isolamento%20Termico_(29-1).pdf)
35. <http://www.celenit.com/prodotti/lana-di-legno/celenit-n>
36. <http://www.ytong.it/it/content/Blocchi%20Ytong.php>
37. prEN 12494, building components and elements—in situ measurement of the surface to surface thermal resistance (1996)
38. C. Buratti, S. Grignaffini, Int. J. Heat Technol. **21** (2003)
39. A.M. Papadopoulos, Energy Build. **37**, 77 (2005)
40. R. Lollini, G. Barozzi, G. Fasano, I. Meroni, M. Zinzi, Build. Environ. **41**, 1001 (2006)